

See discussions, stats, and author profiles for this publication at: <https://www.researchgate.net/publication/281289513>

The mixed serotonin receptor agonist psilocybin reduces threat-induced modulation of amygdala connectivity

ARTICLE in CLINICAL NEUROIMAGING · AUGUST 2015

Impact Factor: 2.53 · DOI: 10.1016/j.clin.2015.08.009

READS

177

6 AUTHORS, INCLUDING:



André Schmidt

King's College London

54 PUBLICATIONS 313 CITATIONS

[SEE PROFILE](#)



Karl J Friston

University College London

946 PUBLICATIONS 125,624 CITATIONS

[SEE PROFILE](#)



Katrin Preller

University of Zurich/ University College Lon...

37 PUBLICATIONS 247 CITATIONS

[SEE PROFILE](#)

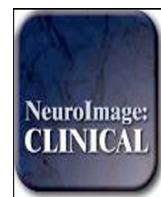


Franz X. Vollenweider

University of Zurich

188 PUBLICATIONS 6,864 CITATIONS

[SEE PROFILE](#)



Q1 The mixed serotonin receptor agonist psilocybin reduces threat-induced 2 modulation of amygdala connectivity

3 Rainer Kraehenmann^{a,b,*}, André Schmidt^{c,d}, Karl Friston^e, Katrin H. Preller^b,
4 Erich Seifritz^a, Franz X. Vollenweider^b

5 ^aDepartment of Psychiatry, Psychotherapy and Psychosomatics, Psychiatric Hospital, University of Zurich, Zürich 8032, Switzerland

6 ^bNeuropsychopharmacology and Brain Imaging, Department of Psychiatry, Psychotherapy and Psychosomatics, Psychiatric Hospital, University of Zurich, Zürich 8032, Switzerland

7 ^cDepartment of Psychiatry (UPK), University of Basel, Basel 4012, Switzerland

8 ^dDepartment of Psychosis Studies, Institute of Psychiatry, Psychology and Neuroscience, King's College London, London SE5 8AF, United Kingdom

9 ^eWellcome Centre for Imaging Neuroscience, University College London, London WC1N 3BG, United Kingdom

10 ARTICLE INFO

11 Article history:

12 Received 16 June 2015

13 Received in revised form 27 July 2015

14 Accepted 17 August 2015

15 Available online xxxx

16 Keywords:

17 Serotonin

18 Psilocybin

19 Depression

20 fMRI

21 Dynamic causal modeling

ABSTRACT

Stimulation of serotonergic neurotransmission by psilocybin has been shown to shift emotional biases away from negative towards positive stimuli. We have recently shown that reduced amygdala activity during threat processing might underlie psilocybin's effect on emotional processing. However, it is still not known whether psilocybin modulates bottom-up or top-down connectivity within the visual-limbic-prefrontal network underlying threat processing. We therefore analyzed our previous fMRI data using dynamic causal modeling and used Bayesian model selection to infer how psilocybin modulated effective connectivity within the visual-limbic-prefrontal network during threat processing. First, both placebo and psilocybin data were best explained by a model in which threat affect modulated bidirectional connections between the primary visual cortex, amygdala, and lateral prefrontal cortex. Second, psilocybin decreased the threat-induced modulation of top-down connectivity from the amygdala to primary visual cortex, speaking to a neural mechanism that might underlie putative shifts towards positive affect states after psilocybin administration. These findings may have important implications for the treatment of mood and anxiety disorders.

© 2015 Published by Elsevier Inc. This is an open access article under the CC BY-NC-ND license (<http://creativecommons.org/licenses/by-nc-nd/4.0/>).

40 1. Introduction

41 Serotonin (5-hydroxytryptamine, 5-HT) is an important neurotransmitter within neural networks related to emotion processing.
42 We have recently shown that 5-HT2A receptor activation by psilocybin (4-phosphoryloxy-N,N-dimethyltryptamine) attenuates amygdala activation in response to threat-related visual stimuli in healthy volunteers and that the reduction of amygdala blood oxygen level-dependent (BOLD) signal is related to psilocybin's mood-enhancing effect (Kraehenmann et al., 2014). Here, we addressed the hypothesis that connectivity changes between the amygdala (AMG) and visual and prefrontal cortical (PFC) areas contribute to the observed effects of psilocybin on threat processing previously observed (Kraehenmann et al., 2014). This hypothesis is based on evidence showing that the

processing of threat-related visual stimuli may be modulated via feedback connections from the amygdala to the visual cortex (Furl et al., 2013). Such top-down input from the amygdala to the visual cortex may be an important mechanism at the interface between emotion processing and visual perception – given that the amygdala has been implicated in tuning visual processing to allocate resources towards sensory processing of – and coordinating responses to – emotionally salient stimuli (Morris et al., 1998). Furthermore, processing of threat signals may be modulated via inhibitory feedback connections from the PFC to the AMG (Hahn et al., 2011; Aznar and Klein, 2013). Using DCM for fMRI, Sladky et al. (2015) recently analyzed the effects of the selective serotonin reuptake inhibitor (SSRI) (S)-citalopram on amygdala-PFC effective connectivity in healthy volunteers. They found that the PFC exhibited a down-regulatory effect on amygdala activation, and that this effect was significantly increased by the antidepressant (S)-citalopram. Importantly, the inhibitory feedback from the PFC to the AMG has been found to be correlated with 5-HT2A receptor stimulation (Fisher et al., 2009). Therefore, it is conceivable that the psilocybin-induced attenuation of amygdala activation (Kraehenmann et al., 2014)

* Corresponding author at: Neuropsychopharmacology and Brain Imaging, Department of Psychiatry, Psychotherapy and Psychosomatics, Psychiatric Hospital, University of Zurich, Lenggstrasse 31, Zürich CH-8032, Switzerland. Tel.: +41 44 384 2827.

E-mail address: r.kraehenmann@bli.uzh.ch (R. Kraehenmann).

72 might be caused by increased inhibitory connectivity from the PFC to the
 73 AMG. Finally, given the abundance of feed-forward projections from
 74 visual input regions (e.g. primary visual cortex, V1) to the AMG (Pessoa
 75 and Adolphs, 2010) and from the AMG to the PFC (Volman et al., 2013),
 76 bottom-up connectivity changes may also contribute to psilocybin's
 77 effects on threat processing.

To test these hypotheses, we analyzed the functional magnetic resonance imaging (fMRI) data of our previous study (Kraehenmann et al., 2014) using dynamic causal modeling (DCM) (Friston et al., 2003) and Bayesian model selection (BMS) (Stephan et al., 2009). DCM is a general framework for inferring hidden mechanisms at the neuronal level from measurements of brain activity such as fMRI. Recent studies have demonstrated its sensitivity to detect pharmacological manipulations in fMRI data (Grefkes et al., 2010; Schmidt et al., 2013b); in particular, after serotonergic stimulation (Volman et al., 2013). BMS is an essential aspect of DCM studies, as it can be used to test competing hypotheses (different DCMs) about the neural mechanisms generating data. We applied DCM and BMS to address the following questions: First, which is the most likely mechanism underlying threat processing, (1) threat-induced modulation of bottom-up connectivity, (2) threat-induced modulation of top-down connections, or (3) modulation of both bottom-up and top-down connections by threat stimuli. Secondly, which of these mechanisms – changes in bottom-up or top-down connectivity – contributed to the psilocybin-induced reduction of AMG (Kraehenmann et al., 2014) and V1 activation (Schmidt et al., 2013a) in response to threat-related visual stimuli.

98 2. Methods

99 2.1. Subjects

100 In total, 25 healthy, right-handed subjects (16 males, mean age
 101 24.2 ± 3.42 years) with normal or corrected-to-normal vision were re-
 102 cruited through advertisements placed in local universities. Subjects
 103 were screened for DSM-IV mental and personality disorders using the
 104 Mini-International Neuropsychiatric Interview (Sheehan et al., 1998)
 105 and the Structured Clinical Interview II (First et al., 1997). Exclusion
 106 criteria were as follows: pregnancy, left-handedness, poor knowledge
 107 of the German language, personal or first-degree relatives with history
 108 of psychiatric disorder, history of alcohol or illicit drug dependence,
 109 current alcohol abuse or illicit drug use, current use of a medication
 110 that affects cerebral metabolism or blood flow, cardiovascular disease,
 111 history of head injury or neurological disorder, magnetic resonance im-
 112 aging exclusion criteria (including claustrophobia), and previous signif-
 113 icant adverse reactions to a hallucinogenic drug. Subjects were healthy
 114 according to medical history, physical examination, routine blood anal-
 115 ysis, electrocardiography, and urine tests for drug abuse and pregnancy.
 116 The study was approved by the Cantonal Ethics Committee of Zurich
 117 (KEK). Written informed consent was obtained from all subjects and
 118 the study was performed in accordance with the Declaration of Helsinki.

119 2.2. Experimental design

120 As previously reported (Kraehenmann et al., 2014), the study design
 121 was randomized, double-blind, placebo-controlled, cross-over. Subjects
 122 received either placebo or 0.16 mg/kg oral psilocybin in two separate
 123 imaging sessions at least 14 days apart. The use of psilocybin was auth-
 124 orized by the Federal Office of Public Health, Federal Department of
 125 Home Affairs, Bern, Switzerland. Psilocybin and lactose placebo were
 126 administered in gelatin capsules of identical number and appearance.
 127 A 0.16-mg/kg dose of psilocybin was selected because it reliably induces
 128 changes in mood and consciousness, but minimally disrupts behavioral
 129 task performance and reality testing (Studerus et al., 2011). Mood state
 130 was assessed using the Positive and Negative Affect Schedule
 131 (PANAS) (Watson et al., 1988) and the state portion of the State-Trait

Anxiety Inventory (STAI) (Spielberger and Gorsuch, 1983) before and 132 210 min after each drug treatment. The scanning experiment was con- 133 ducted between 70 and 90 min after drug administration to coincide 134 with the plateau in the subjective effects of psilocybin (Hasler et al., 135 2004). Subjects were released about 360 min after drug administration, 136 after all acute drug effects had completely subsided. 137

138 2.3. fMRI paradigm: amygdala reactivity task

Inside the scanner, subjects performed an amygdala reactivity task 139 comprising alternating blocks of emotional (threat and neutral) picture 140 discrimination tasks. The picture discrimination task was interspersed 141 with shape discrimination tasks, which served as baseline tasks and 142 allowed amygdala responses to return to baseline. 143

Stimulus material for the amygdala reactivity task was obtained 144 from the International Affective Picture System (IAPS), a standardized 145 and broadly validated collection of emotionally evocative pictures 146 (Lang et al., 2005). Stimulus sets of 48 different pictures were arranged 147 in picture-triplets on a gray background. The stimulus triplets com- 148 prised the target picture in the upper center position, and two pictures 149 as potential matching targets on the left and right sides at the bottom of 150 the slide. Twenty-four pictures were categorized as threat and 24 as 151 neutral. The threat pictures were aversive, threat-related pictures such 152 as attacking animals, aimed weapons, car accidents, and mutilations, 153 and the neutral pictures depicted activities of daily living, portraits of 154 humans and animals, and everyday objects. 155

During the emotional picture discrimination task, subjects were re- 156 quired to select one of the two IAPS pictures at the bottom of the stim- 157 ulus triplet that matched the target picture at the top of the triplet. 158 Selection was indicated by pressing one of two buttons on a magnetic 159 resonance (MR)-compatible response device with the dominant hand. 160 A shape discrimination task was performed as a sensorimotor control 161 and baseline task. This required matching of geometric shapes (circles, 162 ovals, and rectangles) analogous to the picture discrimination task and 163 was implemented to control for activation due to non-emotional cogni- 164 tive and visual processing. Both tasks were shown as alternating 24-s 165 blocks without intermittent pauses. Each block was preceded by a 2-s 166 instruction ("Match Pictures" or "Match Forms") and consisted of six 167 target images that were presented sequentially for a period of 4 s in a 168 randomized order. The experimental design comprised four repetitions 169 of the sequence threat → shapes → neutral → shapes, cumulating to a 170 total duration of 420 s for the complete run. Individual trial durations 171 were not determined by the subjects' responses, and no feedback was 172 provided regarding correct or incorrect responses. 173

174 2.4. fMRI image acquisition and data analysis

Scanning was performed on a 3 T scanner (Philips Achieva, Best, The 175 Netherlands) using an echo planar sequence with 2.5 s repetition time, 176 30 ms echo time, a matrix size of 80×80 and 40 slices without inter- 177 slice gap, providing a resolution of $3 \times 3 \times 3 \text{ mm}^3$ and a field of view 178 of $240 \times 240 \text{ mm}^2$. 179

Data analysis was performed with SPM12b (<http://www.fil.ion.ucl.ac.uk>). All volumes were realigned to the mean volume, co-registered 180 to the structural image, normalized to the Montreal Neurological Insti- 181 tute space using unified segmentation (Ashburner and Friston, 2005) 183 including re-sampling to $3 \times 3 \times 3 \text{ mm}$ voxels, and spatially smoothed 184 with an 8-mm full-width at half-maximum Gaussian kernel. First-level 185 analysis was conducted using a general linear model applied to the 186 time series, convolved with a canonical hemodynamic response func- 187 tion (Friston et al., 1994). Serial correlations and low-frequency signal 188 drift were removed using an autoregressive model and a 128-s 189 high-pass filter, respectively. Single-subject GLM analysis for the two 190 sessions (placebo and psilocybin) comprised regressors for threat, neu- 191 tral pictures, and shapes. These conditions were modeled as box-car 192

193 regressors representing the onset of each block type. Subject-specific
 194 condition effects for threat minus shapes were computed using
 195 t-contrasts, producing a contrast image for each subject that was used
 196 as a summary statistic for second-level (between subject) analyses.

197 2.5. Dynamic causal modeling (DCM)

198 The current DCM analyses (version 12 with SPM12b) are based on
 199 the GLM analyses of the fMRI data described above (Kraehenmann
 200 et al., 2014). In DCM for fMRI, the dynamics of the neural states under-
 201 lying regional BOLD responses are modeled by a bilinear differential
 202 equation that describes how the neural states change as a function of
 203 endogenous interregional connections, modulatory effects on these
 204 connections, and driving inputs (Friston et al., 2003). The endogenous
 205 connections represent constant coupling strengths, whereas the
 206 modulatory effects represent context-specific and additive changes in
 207 coupling (task-induced alterations in connectivity). The modeled
 208 neuronal dynamic is then mapped to the measured BOLD signal using
 209 a hemodynamic forward model (Stephan et al., 2007). We explicitly
 210 examined how the coupling strengths between V1, AMG, and PFC are
 211 changed by threat during the AMG reactivity task (modulatory effect).

212 2.5.1. Regions of interest and time series extraction

213 We selected three regions of interest (ROIs) within a right-
 214 hemispheric network implicated in visual threat processing, based on:
 215 (1) previously published conventional SPM analyses of these data
 216 (Fig. 1) (Kraehenmann et al., 2014), (2) previous anatomical and struc-
 217 tural connectivity studies (Freese and Amaral, 2005), and (3) previous
 218 DCM studies of threat processing using visual stimuli (Volman et al.,
 219 2013). In DCM for fMRI, a neural network is analyzed in terms of direct-
 220 ed connectivity changes among selected regions of interest. Regions of
 221 interest are selected based on both a priori knowledge and hypotheses,
 222 and on significant task-induced activations. We chose a right-
 223 hemispheric (subgraph) analysis based on our previous GLM analysis
 Q2 of psilocybin effects on threat processing (see Table 1, Fig. 3A and B)
 225 (Kraehenmann et al., 2014). The rationale for this choice was to ask
 226 whether the observed psilocybin-induced decrease of right amygdala
 227 activation in response to threat was mediated by top-down connectivity
 228 changes from the right prefrontal cortex or by bottom-up connectivity
 229 changes from the right visual cortex. In addition, we limited our DCM
 230 analyses to a right-hemispheric network or subgraph in view of statisti-
 231 cal efficiency: it is common practice to test only a small number of
 232 regions of interest with DCM. Future DCM studies of psilocybin effects
 233 on threat processing could include the contralateral homologues of
 234 the regions investigated here, although our previous GLM analysis did
 235 not motivate a DCM analysis of the left-hemispheric network.

236 The ROIs included: rV1 ($x = 12, y = -82, z = -7$), rAMG ($x = 24,$
 237 $y = -1, z = -13$), and the right inferior frontal gyrus within the lateral
 238 PFC (rLPFC) ($x = 54, y = 32, z = 20$). The coordinates for the rV1, rAMG
 239 and rLPFC were based on the contrast of threat pictures minus shapes.

240 Regional time series from each subject and session were extracted from
 241 (10 mm) spherical volumes of interest centered on the suprathreshold
 242 voxel nearest the group maxima. Time series were summarized with
 243 the first eigenvariate of voxels above a subject-specific F threshold of
 244 $p < 0.01$ (uncorrected) within the anatomical areas, as defined by the
 245 Pick Atlas toolbox. During time series extraction it may happen that a
 246 subject does not show activation at the group maximum and that the
 247 nearest suprathreshold voxel lies outside the anatomical regions. By
 248 additionally using an anatomical mask, we ensured that time series
 249 were extracted from within a certain distance of the group maxima
 250 (10 mm), but were not extracted from a region outside the anatomical
 251 structure (Dima et al., 2011). We could not extract an rLPFC time series
 252 in two subjects due to lack of individual activations fulfilling both the
 253 above functional and anatomical criteria. Although it is not necessary to
 254 preclude subjects who did not show significant activations from the
 255 DCM analysis, the purpose of DCM is to explain observed activations in
 256 terms of functional coupling. We therefore restricted our analyses to sub-
 257 jects who showed significant responses under the assumption that their
 258 data would provide more efficient estimators of connectivity. 259

260 2.5.2. DCM model space

261 First, we specified a three-area base model with bidirectional endog-
 262 enous connections between V1 and AMG and between AMG and LPFC
 263 (Fig. 2A). V1 was selected as the visual input region in our models. All
 264 visual stimuli were used as inputs. These restrictions allowed us to
 265 define a small model space. The basic model was then systematically
 266 varied to provide alternative models of the modulatory effect (induced
 267 by threat stimuli). The three model variants corresponded to the
 268 three alternative hypotheses about modulatory effects (bottom-up,
 269 top-down, or a combination of bottom-up and top-down) and allowed
 270 us to distinguish between the three hypothesized mechanisms under
 271 the two treatments (psilocybin, placebo) (Fig. 2B–D). 272

273 2.5.3. Model inference

274 Using random-effects BMS in DCM12, we computed expected prob-
 275 abilities and exceedance probabilities at the group-level to determine
 276 the most plausible of the three model variants for each drug (psilocybin,
 277 placebo) separately (Penny et al., 2004). The expected probability of
 278 each model is the probability that a specific model generated the data
 279 of a randomly chosen subject, and the exceedance probability of each
 280 model is the probability that this model is more likely than any other
 281 of the models tested (Stephan et al., 2009). Bayesian model comparison
 282 rests solely on the relative evidence for different models (as scored by
 283 the variational free energy). This evidence comprises the accuracy
 284 (i.e., percent variance explained) minus the complexity (i.e., degrees
 285 of freedom used to explain the data). The evidence therefore reflects
 286 the quality of a model in providing an accurate but parsimonious ac-
 287 count of the data (and is preferred over conventional accuracy measures
 288 that may reflect overfitting). Finally, we used random-effects Bayesian
 289 model averaging (BMA) to compute (subject specific) connectivity 290

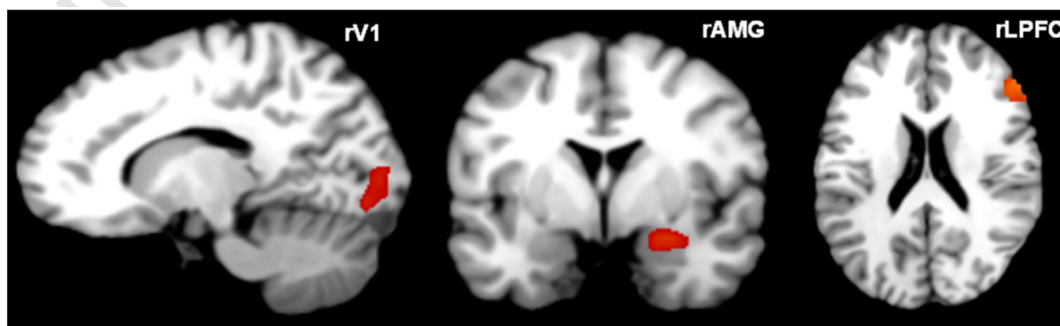


Fig. 1. Regional effects from the contrast of threat pictures minus shapes within right lateral prefrontal cortex (rLPFC; $z = 20$) and right amygdala (rAMG; $y = -1$) and from the contrast of all pictures (threat of non-threat) minus shapes within the right primary visual cortex (rV1; $x = 12$) across both drug conditions (placebo, psilocybin). SPM(t) overlaid on canonical brain slices (thresholded at $p < 0.001$ uncorrected for visualization).

Table 1
Dynamic causal modeling parameter estimates.

Connection	Endogenous		Modulation		Direct input	
	Pla	Psi	Pla	Psi	Pla	Psi
V1	+0.023 ± 0.05	-0.002 ± 0.01	-	-	+0.011 ± 0.12	-0.003 ± 0.01
V1 → AMG	+0.036 ± 0.08	+0.018 ± 0.05	+0.027 ± 0.37	+0.024 ± 0.09	-	-
AMG → V1	-0.028 ± 0.09	+0.031 ± 0.11	+0.526 ± 1.05	+0.030 ± 0.14*	-	-
AMG	-0.007 ± 0.02	-0.002 ± 0.01	-	-	-	-
AMG → LPFC	+0.005 ± 0.08	-0.005 ± 0.06	+0.103 ± 0.22	+0.023 ± 0.11	-	-
LPFC → AMG	-0.002 ± 0.05	+0.008 ± 0.00	-0.394 ± 1.12	-0.157 ± 0.76	-	-
LPFC	-0.014 ± 0.04	-0.001 ± 0.00	-	-	-	-

estimates (weighted by their posterior model probability) across all three models separately for psilocybin and placebo. This conservative analysis allowed the drug effect to be expressed in all connections and their threat related modulations, whereby we were able to establish significant effects in relation to intersubject variability using classical statistics at the between subject level.

2.5.4. Parameter inference

To evaluate the effect of psilocybin on endogenous connections and their modulation by threat stimuli, BMA values were entered into two separate 2-way repeated measures ANOVA with factors drug (psilocybin, placebo) and connection type (endogenous parameters: V1, V1 → AMG, AMG → V1, AMG, AMG → LPFC, LPFC → AMG, LPFC; modulatory parameters: V1 → AMG, AMG → V1, AMG → LPFC, LPFC → AMG). Where the ANOVA null hypothesis of equal means was rejected, we used the post-hoc test (Duncan's multiple range tests). A paired t test was further applied to compare direct inputs into V1 across both treatments. A p value of less than 0.05 was assumed as statistically significant.

2.5.5. Correlation with behavioral and mood measures

To investigate correlations between psilocybin-induced changes of effective connectivity and behavior or mood, the psilocybin-induced connectivity changes were correlated using Pearson correlations with

psilocybin-induced changes in behavioral measures (reaction time, accuracy) and mood scores (PANAS positive affect, PANAS negative affect, STAI state anxiety).

3. Results

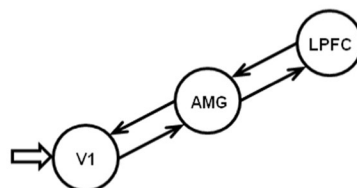
3.1. Model inference with Bayesian model selection

Under both psilocybin and placebo, the full model outperformed all other models with an exceedance probability of 97% (placebo) and 62% (psilocybin), respectively (Fig. 3). This optimal model comprised bidirectional endogenous connections between V1 and AMG, and between AMG and LPFC, with threat modulating both forward and backward connections.

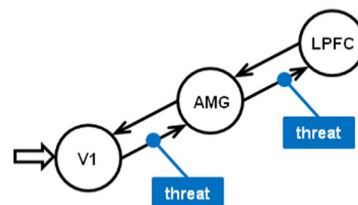
3.2. Parameter inference

To compare connectivity across drug treatments, the subject-specific parameter estimates were averaged over the three models for each treatment using BMA. The endogenous parameters, their threat induced modulations, and direct inputs from the BMA are shown in Table 1. Coupling or connectivity in dynamic models is measured in terms of Hz, where a strong baseline or endogenous connection would typically be between 0.1 and 0.5 Hz. This means that one can regard the effective connectivity as a rate-constant. In other words, a strong connection

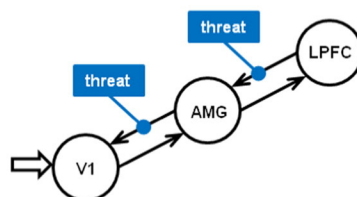
A: base model



B: bottom-up model



C: top-down model



D: full model

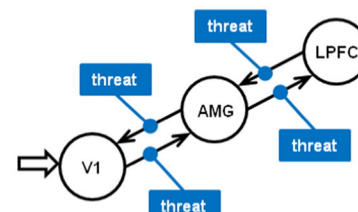


Fig. 2. Model specification. A, Basic structure of the three-area model: visual stimulus presentation drives V1 activity, which is bidirectionally connected to AMG, which in turn is bidirectionally connected to the LPFC. B, Bottom-up model: the modulatory effect of threat is only mediated via bottom-up connections from V1 to AMG to LPFC. C, Top-down model: the modulatory effect of threat is only mediated via top-down connections from LPFC to AMG to V1. D, Full model: the modulatory effect of threat is mediated via both bottom-up and top-down connections between V1 and AMG, and between AMG and LPFC.

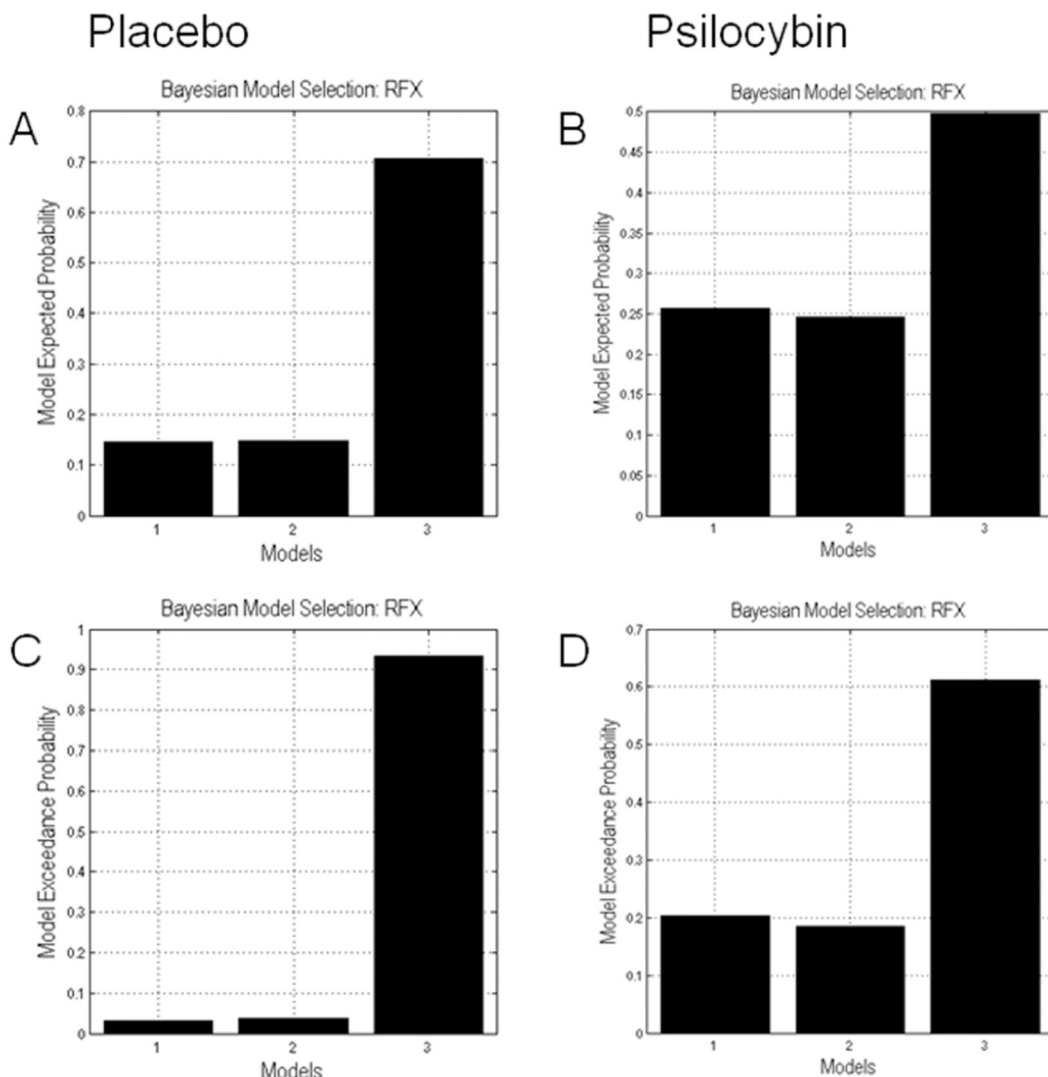


Fig. 3. Results of Bayesian model selection. Bar charts show the expected model probabilities (A, B) and exceedance probabilities (C, D) of the bottom-up model (1), the top-down model (2), and the full model (3) for the placebo (left) and psilocybin (right) treatment. Notably, the full model with threat-induced modulation of bidirectional connections is the winning model for both the placebo and psilocybin treatment.

330 causes a large rate of increase in the target region, with respect to
 331 activity in the source region. The inverse of the connection strength
 332 can therefore be interpreted in terms of a time constant (i.e., how long
 333 it would take for a source to increase activity in a target).

334 There was no main effect of drug ($F_{1,22} = 3.10, p = 0.09, \eta_p^2 = 0.12$),
 335 but a significant main effect of connection type ($F_{3,66} = 3.94, p = 0.01,$
 336 $\eta_p^2 = 0.15$), and a significant drug by connection type interaction
 337 ($F_{3,66} = 2.84, p = 0.04, \eta_p^2 = 0.11$) on modulatory coupling parameters.
 338 Post-hoc tests on the drug by connection type interaction showed that
 339 the threat-induced modulation of AMY → V1 connectivity was signifi-
 340 cantly reduced after psilocybin compared to placebo administration
 341 ($p = 0.01$; Duncan's multiple range test corrected) (Table 1). There
 342 was no significant effect of psilocybin on endogenous or input parame-
 343 ters (all $p > 0.05$).

344 Parameter estimates were obtained from Bayesian Model Averaging
 345 for placebo (Pla) and psilocybin (Psi), mean \pm standard deviation.
 346 Statistically significant differences between placebo and psilocybin
 347 treatments ($p < 0.05$ Duncan corrected for multiple comparison) are
 348 printed in bold and marked by an asterisk; V1 = primary visual cortex;
 349 AMG = amygdala; LPFC = lateral prefrontal cortex.

3.3. Correlation with behavioral and mood measures

We assessed correlations between (psilocybin–placebo) modulatory 351
 coupling changes for the AMG → V1 connection from BMA and (psilocy- 352
 bin–placebo) changes of behavioral measures (reaction time, accuracy) 353
 and of mood scores (PANAS positive affect, PANAS negative affect, STAI 354
 state anxiety). We found no significant correlations (all $p > 0.05$). 355

4. Discussion

In this study, we analyzed the fMRI data of our previous psilocybin 357
 study (Kraehenmann et al., 2014) using DCM, an established framework 358
 enabling tests of directed (effective) connectivity. We were interested 359
 whether psilocybin modulated effective connectivity within a network 360
 implicated in threat processing during an amygdala reactivity task. In 361
 particular, our aim was to differentiate between psilocybin-effects on 362
 bottom-up, top-down, and bidirectional connectivity during threat- 363
 processing within a visual–limbic–prefrontal network. There were two 364
 main findings from our study: Firstly, both placebo and psilocybin 365
 data were best explained by a model in which threat affect modulated 366

367 bidirectional connections between V1, AMG, and LPFC. Secondly,
 368 psilocybin – compared to placebo – substantially reduced the modulatory
 369 effect of threat on the top-down connection from the AMG to V1. This
 370 implies that psilocybin attenuates amygdala-dependent top-down
 371 tuning of visual regions during threat processing.

372 Our BMS finding that the full model, which is characterized by bidi-
 373 rectional modulatory effects of threat on visual-limbic-prefrontal con-
 374 nectivity, outperformed both the bottom-up and the top-down model,
 375 is in line with previous DCM studies (Herrington et al., 2011; Goulden
 376 et al., 2012). In these studies, BMS consistently favored models, which
 377 implement modulatory effects on both bottom-up and top-down con-
 378 nections during negative emotion processing. The winning model in
 379 our study contained reciprocal connections between V1 and AMG
 380 ($V1 \leftrightarrow AMG$) and between AMG and LPFC ($AMG \leftrightarrow LPFC$). Both
 381 $V1 \leftrightarrow AMG$ and $AMG \leftrightarrow LPFC$ reciprocal connections are critically in-
 382 volved in negative-emotion processing (Herrington et al., 2011;
 383 Goulden et al., 2012). In fact, it has been shown that visual threat
 384 perception may be enhanced through a re-entry mechanism of feed-
 385 forward connections from V1 to AMG and feedback connections from
 386 the AMG to V1 (Herrington et al., 2011). Furthermore, visual threat
 387 perception may be increased through feed-forward connections from
 388 the AMG to LPFC (Lu et al., 2012) and attenuated through inhibitory
 389 feedback connections from the LPFC to AMG (Volman et al., 2013). Al-
 390 though BMS did not directly compare model fits from different datasets
 391 (e.g. placebo, psilocybin), our model selection results indicate a consis-
 392 tent mode of visual threat processing during placebo and psilocybin
 393 treatments; namely, via modulation of both bottom-up and top-down
 394 connectivity across the visual-limbic-prefrontal hierarchy.

395 Our main finding was that psilocybin (compared to placebo)
 396 reduced the modulatory effect of visual threat on the top-down connec-
 397 tion from the AMG to V1. In both humans and animals, visual threat
 398 poses a strong salience signal, which needs to be processed efficiently
 399 and therefore binds attentional resources (Pessoa and Adolphs, 2010).
 400 The “tuning” of visual regions via feedback projections from the AMG
 401 during threat processing is an important mechanism underlying visual
 402 threat processing and may enhance perception of visual threat signals
 403 (Morris et al., 1998). In addition, the AMG has been closely linked to
 404 salience processing and may, via top-down predictive signals, guide
 405 bottom-up information processing (Vuilleumier, 2015). Therefore, the
 406 amygdala may actually determine the affective meaning of visual
 407 percepts by its effects on sensory pathways – an effect which mainly
 408 occurs subconsciously and which may be greatly amplified in psycho-
 409 pathological conditions, such as anxiety disorders or depression. In
 410 this context, increased AMG reactivity may lead to an increased
 411 attentional focus on negatively valenced environmental or social stimuli
 412 and thus effectively blocks out the processing of positive information
 413 (Disner et al., 2011). This is especially relevant for hallucinogenic
 414 drugs such as psilocybin, because there has been a close and psycho-
 415 therapeutically interesting relationship between visual perception and
 416 affective processes during hallucinogen-induced states (Leuner, 1981).
 417 The psilocybin-induced attenuation of top-down threat signaling from
 418 the amygdala to visual cortex may therefore lead to decreased threat
 419 sensitivity in the visual cortex. This mechanism may crucially underlie
 420 the previously observed decrease of behavioral and electrophysiological
 421 responses in the visual cortex to threat stimuli during psilocybin
 422 administration (Vollenweider and Kometer, 2010; Schmidt et al.,
 423 2013a) and may explain the psilocybin-induced shifts away from
 424 negative towards positive valence during emotion processing
 425 (Kometer et al., 2012). In line with the notion that attenuation of the
 426 top-down connection from the AMG to visual cortex may reduce threat
 427 processing, a recent study showed that habituation to visual threat
 428 stimuli may parallel attenuation of top-down connectivity from the
 429 AMG to visual cortex (Herrington et al., 2011). In addition, it has been
 430 found that hyper-connectivity between the AMG and visual cortex
 431 may underlie increased threat processing and anxiety (Frick et al.,
 432 2013).

Given the relevance of LPFC in regulating AMG activity during threat processing, and given previous studies showing that serotonergic stimulation may increase inhibitory top-down connectivity from LPFC to AMG (Pessoa and Adolphs, 2010; Volman et al., 2013), we hypothesized that psilocybin-induced reduction in AMG activity might be due to an increased LPFC → AMG top-down connectivity during threat processing. However, psilocybin did not appear to increase top-down connectivity from LPFC to AMG in the current analysis. Two reasons might account for this. First, the source of the psilocybin-induced reduction of AMG activity, as observed in our previous GLM analysis (Kraehenmann et al., 2014), might not reflect an increased top-down effect from LPFC, but rather a suppression of recurrent interactions with visual areas mediated by a reduced top-down connectivity with the visual cortex. The synaptic basis of this reduced top-down modulation might reflect a direct effect of psilocybin in the amygdala: amygdala neurons abundantly express 5-HT2A receptors, and DOI and other 5-HT2A agonists produce direct effects in the amygdala (Rainnie, 1999). In addition, a directly decreased AMG reactivity would result in a reduced load on the LPFC to regulate AMG activation. This view is supported by a recent DCM study showing that increased AMG-related load on the PFC yields subsequent responses in the PFC to regulate the AMG (Volman et al., 2013). Second, the AMG might be regulated by prefrontal cortical regions other than the LPFC, such as the medial PFC (MPFC), the anterior cingulate cortex (ACC), or the orbitofrontal cortex (OFC), which have also been related to the ‘aversive amplification’ circuit (Robinson et al., 2013). For example, Sladky et al. (2015) recently analyzed the effects of the selective serotonin reuptake inhibitor (SSRI) (S)-citalopram on amygdala-OFC effective connectivity in healthy volunteers. They found that the OFC exhibited a down-regulatory effect on amygdala activation, and that this effect was significantly increased by the antidepressant (S)-citalopram. Although Sladky et al. used a similar threat-inducing amygdala reactivity task (Hariri et al., 2002) and likewise tested the effects in healthy volunteers, their study procedures differ substantially from our study, both in terms of task design (e.g. face stimuli instead of pictures, scrambled control stimuli, longer baseline conditions) and in terms of drug administration (e.g. chronic and repeated instead of acute and single treatment). Therefore, it is not easy to disambiguate task- from drug-specific effects in terms of PFC involvement and our DCM might have missed top-down effects from PFC on the AMG. However, given the cognitive task requirements in our task – where subjects were not explicitly required to evaluate or regulate their emotional responses to the threat stimuli – and given that the GLM analyses (Kraehenmann et al., 2014) did not show significant BOLD responses in the MPFC, ACC, or OFC, one might argue that top-down effects from other prefrontal regions are unlikely. Overall, both the hallucinogen psilocybin and the non-hallucinogen (S)-citalopram may normalize amygdala hyper-reactivity to threat-related stimuli; leading to their antidepressant and anxiolytic efficacy, but psilocybin appears to regulate emotion processing and mood by acting on network interactions which are different from classical antidepressants such as (S)-citalopram, such as the affective regulation of visual information processing shown here.

4.1. Limitations and future directions

There are some limitations to be considered in the present study. We used a fairly simplistic neuronal network underlying threat related effective connectivity. There are also other brain regions involved in threat processing, such as the ACC, the OFC, or the fusiform gyrus (Robinson et al., 2013), but that we did not include in our present model for reasons of parsimony and based on our *a priori* hypotheses. Furthermore, to maximize statistical efficiency, we only considered right-hemispheric networks in our DCM analyses. Therefore, top-down connectivity from the left LPFC to the right AMG might have been missed. Given the importance of the left LPFC in regulating the right AMG during emotion processing and in serotonergic modulation

497 (Outhred et al., 2013), we cannot exclude this possibility. Therefore, further effective connectivity studies using tasks that differentially recruit
 498 left and right prefrontal cortical regions during threat processing, are
 499 needed.
 500

501 4.2. Conclusion

502 This effective connectivity study shows that a decrease of top-down
 503 connectivity from the AMG to the visual cortex underlies the psilocybin
 504 effect on visual threat processing. This result suggests that decreased
 505 threat sensitivity in the visual cortex during emotion processing may
 506 explain the potential of psilocybin to acutely shift emotional biases
 507 away from negative towards positive valence: the capacity of the visual
 508 cortex to process multiple stimuli is limited and hence top-down sup-
 509 pression of negative stimuli enhances the processing of positive stimuli
 510 (Kastner et al., 1998). This may have important therapeutic implications
 511 for mood and anxiety disorders, where over-loading with negative
 512 stimuli and persistence of negative cognitive biases is a central feature
 513 (Disner et al., 2011). In post-traumatic stress disorder, for example,
 514 psilocybin might help inhibit fear-responses during exposure-based
 515 psychotherapy, which might facilitate therapeutic progress.

516 Disclosure and conflict of interest

517 This work was supported by grants from the Swiss Neuromatrix
 518 Foundation, Switzerland and the Heffter Research Institute, USA; and
 519 by the Swiss National Science Foundation (A.S., No. 155184); K.F. was
 520 funded by a Wellcome Trust Principal research fellowship (Ref:
 521 088130/Z/09/Z). The authors report no biomedical financial interests
 522 or potential conflicts of interest.

523 Acknowledgments

524 We thank the staff at the Department of Psychiatry Psychotherapy
 525 and Psychosomatics for the medical and administrative support.

526 References

Ashburner, J., Friston, K.J., 2005. Unified segmentation. *Neuroimage* 26 (3), 839–851. <http://dx.doi.org/10.1016/j.neuroimage.2005.02.018>[15955494](http://dx.doi.org/10.1016/j.neuroimage.2005.02.018).

Aznar, S., Klein, A.B., 2013. Regulating prefrontal cortex activation: an emerging role for the 5-HT_{2A} serotonin receptor in the modulation of emotion-based actions? *Mol. Neurobiol.* 48 (3), 841–853. <http://dx.doi.org/10.1007/s12035-013-8472-0>[23696058](http://dx.doi.org/10.1007/s12035-013-8472-0).

Dima, D., Stephan, K.E., Roiser, J.P., Friston, K.J., Frangou, S., 2011. Effective connectivity during processing of facial affect: evidence for multiple parallel pathways. *J. Neurosci.* 31 (40), 14378–14385. <http://dx.doi.org/10.1523/JNEUROSCI.2400-11.2011>[1976523](http://dx.doi.org/10.1523/JNEUROSCI.2400-11.2011).

Disner, S.G., Beevers, C.G., Haigh, E.A.P., Beck, A.T., 2011. Neural mechanisms of the cognitive model of depression. *Nat. Rev. Neurosci.* 12 (8), 467–477. <http://dx.doi.org/10.1038/nrn30271731066>.

First, M.B., Gibbon, M., Spitzer, R.L., Williams, J.B.W., Benjamin, L.S., 1997. Structured Clinical Interview for DSM-IV Axis II Personality Disorders (SCID-II). American Psychiatric Press, Inc., Washington, D.C.

Fisher, P.M., Meltzer, C.C., Price, J.C., Coleman, R.L., Ziolko, S.K., Becker, C., Moses-Kolkov, E.L., Berga, S.L., Hariri, A.R., 2009. Medial prefrontal cortex 5-HT_{2A} density is correlated with amygdala reactivity, response habituation, and functional coupling. *Cereb. Cortex* 19 (11), 2499–2507. <http://dx.doi.org/10.1093/cercor/bhp02219321655>.

Freese, J.L., Amaral, D.G., 2005. The organization of projections from the amygdala to visual cortical areas TE and V1 in the macaque monkey. *J. Comp. Neurol.* 486 (4), 295–317. <http://dx.doi.org/10.1002/cne.2052015846786>.

Frick, A., Howne, K., Fischer, H., Kristiansson, M., Furmark, T., 2013. Altered fusiform connectivity during processing of fearful faces in social anxiety disorder. *Transl. Psychiatry* 3, e312. <http://dx.doi.org/10.1038/tp.2013.8524105443>.

Friston, K.J., Harrison, L., Penny, W., 2003. Dynamic causal modelling. *Neuroimage* 19 (4), 1273–1302. [http://dx.doi.org/10.1016/S1053-8119\(03\)00202-7](http://dx.doi.org/10.1016/S1053-8119(03)00202-7)[12948688](http://dx.doi.org/10.1016/S1053-8119(03)00202-7).

Friston, K.J., Holmes, A.P., Worsley, K.J., Poline, J.-P., Frith, C.D., Frackowiak, R.S.J., 1994. Statistical parametric maps in functional imaging: a general linear approach. *Hum. Brain Mapp.* 2 (4), 189–210. <http://dx.doi.org/10.1002/hbm.460020402>.

Furl, N., Henson, R.N., Friston, K.J., Calder, A.J., 2013. Top-down control of visual responses to fear by the amygdala. *J. Neurosci.* 33 (44), 17435–17443. <http://dx.doi.org/10.1523/JNEUROSCI.2992-13.201324174677>.

Goulden, N., McKie, S., Thomas, E.J., Downey, D., Juhasz, G., Williams, S.R., Rowe, J.B., Deakin, J.F.W., Anderson, I.M., Elliott, R., 2012. Reversed frontotemporal connectivity during emotional face processing in remitted depression. *Biol. Psychiatry* 72 (7), 562 604–611. <http://dx.doi.org/10.1016/j.biopsych.2012.04.031>[22682158](http://dx.doi.org/10.1016/j.biopsych.2012.04.031).

Grefkes, C., Wang, L.E., Eickhoff, S.B., Fink, G.R., 2010. Noradrenergic modulation of cortical networks engaged in visuomotor processing. *Cereb. Cortex* 20 (4), 783–797. <http://dx.doi.org/10.1093/cercor/bhp14419687293>.

Hahn, A., Stein, P., Windischberger, C., Weissenbacher, A., Spindelberger, C., Moser, E., Kasper, S., Lanzenberger, R., 2011. Reduced resting-state functional connectivity between amygdala and orbitofrontal cortex in social anxiety disorder. *Neuroimage* 56 (3), 881–889. <http://dx.doi.org/10.1016/j.neuroimage.2011.07.022>[1497657](http://dx.doi.org/10.1016/j.neuroimage.2011.07.022).

Hariri, A.R., Mattay, V.S., Tessitore, A., Kolachana, B., Fera, F., Goldman, D., Egan, M.F., Weinberger, D.R., 2002. Serotonin transporter genetic variation and the response of the human amygdala. *Science* 297 (5580), 400–403. <http://dx.doi.org/10.1126/science.1071829>[12130784](http://dx.doi.org/10.1126/science.1071829).

Hasler, F., Grimbarg, U., Benz, M.A., Huber, T., Vollenweider, F.X., 2004. Acute psychological and physiological effects of psilocybin in healthy humans: a double-blind, placebo-controlled dose-effect study. *Psychopharmacology (Berl.)* 172 (2), 576 145–156. <http://dx.doi.org/10.1007/s00213-003-1640-6>[14615876](http://dx.doi.org/10.1007/s00213-003-1640-6).

Herrington, J.D., Taylor, J.M., Grupe, D.W., Curby, K.M., Schultz, R.T., 2011. Bidirectional communication between amygdala and fusiform gyrus during facial recognition. *Neuroimage* 56 (4), 2348–2355. <http://dx.doi.org/10.1016/j.neuroimage.2011.03.058>[07221497657](http://dx.doi.org/10.1016/j.neuroimage.2011.03.058).

Kastner, S., De Weerd, P., Desimone, R., Ungerleider, L.G., 1998. Mechanisms of directed attention in the human extrastriate cortex as revealed by functional MRI. *Science* 282 (5386), 108–111. <http://dx.doi.org/10.1126/science.282.5386.108>[956472](http://dx.doi.org/10.1126/science.282.5386.108).

Kometer, M., Schmidt, A., Bachmann, R., Studerer, E., Seifritz, E., Vollenweider, F.X., 2012. Psilocybin biases facial recognition, goal-directed behavior, and mood state toward positive relative to negative emotions through different serotonergic subreceptors. *Biol. Psychiatry* 72 (11), 898–906. <http://dx.doi.org/10.1016/j.biopsych.2012.04.005>[00522578254](http://dx.doi.org/10.1016/j.biopsych.2012.04.005).

Kraehenmann, R., Preller, K.H., Scheidegger, M., Pokorny, T., Bosch, O.G., Seifritz, E., Vollenweider, F.X., 2014. Psilocybin-induced decrease in amygdala reactivity correlates with enhanced positive mood in healthy volunteers. *Biol. Psychiatry* 592 592.

Lang, P.J., Bradley, M.M., Cuthbert, B.N., 2005. International affective picture system (IAPS): Affective Ratings of Pictures and Instruction Manual. NIMH, Center for the Study of Emotion & Attention, Gainesville, FL CD-ROM.

Leuner, H., 1981. Halluzinogene. Psychische Grenzzustände in Forschung und Psychotherapie. Hans Huber, Bern, Stuttgart, Wien.

Lu, Q., Li, H., Luo, G., Wang, Y., Tang, H., Han, L., Yao, Z., 2012. Impaired prefrontal-amygdala effective connectivity is responsible for the dysfunction of emotion process in major depressive disorder: a dynamic causal modeling study on MEG. *Neurosci. Lett.* 523 (2), 125–130. <http://dx.doi.org/10.1016/j.neulet.2012.06.05822750155>[601](http://dx.doi.org/10.1016/j.neulet.2012.06.05822750155).

Morris, J.S., Friston, K.J., Büchel, C., Firth, C.D., Young, A.W., Calder, A.J., Dolan, R.J., 1998. A neuromodulatory role for the human amygdala in processing emotional facial expressions. *Brain* 121 (1), 47–57. <http://dx.doi.org/10.1093/brain/121.1.479549487>[604](http://dx.doi.org/10.1093/brain/121.1.479549487).

Outhred, T., Hawkshead, B.E., Wager, T.D., Das, P., Malhi, G.S., Kemp, A.H., 2013. Acute neural effects of selective serotonin reuptake inhibitors versus noradrenaline reuptake inhibitors on emotion processing: implications for differential treatment efficacy. *Neurosci. Biobehav. Rev.* 37 (8), 1786–1800. <http://dx.doi.org/10.1016/j.neubiorev.2013.07.01023886514>[609](http://dx.doi.org/10.1016/j.neubiorev.2013.07.01023886514).

Penny, W.D., Stephan, K.E., Mechelli, A., Friston, K.J., 2004. Comparing dynamic causal models. *Neuroimage* 22 (3), 1157–1172. <http://dx.doi.org/10.1016/j.neuroimage.2004.03.02615219588>[610](http://dx.doi.org/10.1016/j.neuroimage.2004.03.02615219588).

Pessoa, L., Adolphs, R., 2010. Emotion processing and the amygdala: from a 'low road' to 'many roads' of evaluating biological significance. *Nat. Rev. Neurosci.* 11 (11), 614 773–783. <http://dx.doi.org/10.1038/nrn292020959860>[615](http://dx.doi.org/10.1038/nrn292020959860).

Rainnie, D.G., 1999. Serotonergic modulation of neurotransmission in the rat basolateral amygdala. *J. Neurophysiol.* 82 (1), 69–85. <http://dx.doi.org/10.1040/0022-5293-82-1-69>[617](http://dx.doi.org/10.1040/0022-5293-82-1-69).

Robinson, O.J., Overstreet, C., Allen, P.S., Letkiewicz, A., Vytlal, K., Pine, D.S., Grillon, C., 2013. The role of serotonin in the neurocircuitry of negative affective bias: serotonergic modulation of the dorsal medial prefrontal-amygdala 'aversive amplification' circuit. *Neuroimage* 618 78, 217–223. <http://dx.doi.org/10.1016/j.neuroimage.2013.03.0752358742>[621](http://dx.doi.org/10.1016/j.neuroimage.2013.03.0752358742).

Schmidt, A., Kometer, M., Bachmann, R., Seifritz, E., Vollenweider, F., 2013a. The NMDA antagonist ketamine and the 5-HT agonist psilocybin produce dissociable effects on structural encoding of emotional face expressions. *Psychopharmacology (Berl.)* 225 227–239. <http://dx.doi.org/10.1007/s00213-012-2811-0>[022836372](http://dx.doi.org/10.1007/s00213-012-2811-0).

Schmidt, A., Smieskova, R., Aston, J., Simon, A., Allen, P., Fusar-Poli, P., McGuire, P.K., Riecher-Rössler, A., Stephan, K.E., Borgwardt, S., 2013b. Brain connectivity abnormalities predating the onset of psychosis: correlation with the effect of medication. *J.A.M.A. Psychiatry* 70 (9), 903–912. <http://dx.doi.org/10.1001/jamapsychiatry.2013.11723824230>[628](http://dx.doi.org/10.1001/jamapsychiatry.2013.11723824230).

Sheehan, D.V., Lecribier, Y., Sheehan, K.H., Amorim, P., Janavs, J., Weiller, E., Hergueta, T., baker, Dunbar, R., 1998. The Mini-International Neuropsychiatric Interview (M.I.N.I.): the development and validation of a structured diagnostic psychiatric interview for DSM-IV and ICD-10. *Clin. Psychiatry* 59 (Suppl. 20), 22–33. [http://dx.doi.org/10.1016/S0897-4716\(98\)80002-6](http://dx.doi.org/10.1016/S0897-4716(98)80002-6)[634](http://dx.doi.org/10.1016/S0897-4716(98)80002-6).

Sladky, R., Spies, M., Hoffmann, A., Kranz, G., Hummer, A., Gryglewski, G., Lanzenberger, R., Windischberger, C., Kasper, S., 2015. (S)-citalopram Influences Amygdala Modulation in Healthy Subjects: A Randomized Placebo-controlled Double-blind fMRI Study Using Dynamic Causal Modeling 108, pp. 243–250. <http://dx.doi.org/10.1016/j.neuroimage.2015.01.001>[638](http://dx.doi.org/10.1016/j.neuroimage.2015.01.001).

Spielberger, C.D., Gorsuch, R.L., 1983. Manual for the State-Trait Anxiety Inventory (Form Y) ("Self-Evaluation Questionnaire") iv. Consulting Psychologists Press, Palo Alto, CA, p. 36. <http://dx.doi.org/10.1016/j.neuroimage.2009.03.02519306932>[641](http://dx.doi.org/10.1016/j.neuroimage.2009.03.02519306932).

Stephan, K.E., Penny, W.D., Daunizeau, J., Moran, R.J., Friston, K.J., 2009. Bayesian model selection for group studies. *Neuroimage* 46 (4), 1004–1017. <http://dx.doi.org/10.1016/j.neuroimage.2009.03.02519306932>[643](http://dx.doi.org/10.1016/j.neuroimage.2009.03.02519306932).

Stephan, K.E., Weiskopf, N., Drysdale, P.M., Robinson, P.A., Friston, K.J., 2007. Comparing hemodynamic models with DCM. *Neuroimage* 38 (3), 387–401. <http://dx.doi.org/10.1016/j.neuroimage.2007.07.04017884583>[646](http://dx.doi.org/10.1016/j.neuroimage.2007.07.04017884583).

648 Studerus, E., Kometer, M., Hasler, F., Vollenweider, F.X., 2011. Acute, subacute and
649 long-term subjective effects of psilocybin in healthy humans: a pooled analysis of
650 experimental studies. *J. Psychopharmacol. (Oxford)* 25 (11), 1434–1452. <http://dx.doi.org/10.1177/026988111038246620855349>.
651
652 Vollenweider, F.X., Kometer, M., 2010. The neurobiology of psychedelic drugs: implications
653 for the treatment of mood disorders. *Nat. Rev. Neurosci.* 11 (9), 642–651.
654 <http://dx.doi.org/10.1038/nrn288420717121>.
655
656 Volman, I., Verhagen, L., den Ouden, H.E.M., Fernández, G., Rijpkema, M., Franke, B., Toni,
657 I., Roelofs, K., 2013. Reduced serotonin transporter availability decreases prefrontal
658 control of the amygdala. *J. Neurosci.* 33 (21), 8974–8979. <http://dx.doi.org/10.1523/JNEUROSCI.5518-12.201323699508>.
659
660 Vuilleumier, P., 2015. Affective and motivational control of vision. *Curr. Opin. Neurobiol.* 28 (1), 29–35. <http://dx.doi.org/10.1097/WCO.00000000000015925490197>.
661
662 Watson, D., Clark, L.A., Tellegen, A., 1988. Development and validation of brief measures of positive and negative affect: the PANAS scales. *J. Pers. Soc. Psychol.* 54 (6), 662
663 1063–1070. <http://dx.doi.org/10.1037/0022-3514.54.6.10633397865>.
664

UNCORRECTED PROOF